Effect of rod–cone interactions on mesopic visual performance mediated by chromatic and luminance pathways

Andrew J. Zele[1,*], **Michelle L. Maynard**[1], **Daniel S. Joyce**[1], and **Dingcai Cao**[2]

[1]Visual Science Laboratory, School of Optometry and Vision Science & Institute of Health and Biomedical Innovation, Queensland University of Technology, Brisbane, 4059 QLD, Australia

[2]Visual Perception Laboratory, Department of Ophthalmology and Visual Sciences, University of Illinois at Chicago, Chicago 60612, Illinois, USA

Abstract

We studied the effect of rod–cone interactions on mesopic visual reaction time (RT). Rod and cone photoreceptor excitations were independently controlled using a four-primary photostimulator. It was observed that (1) lateral rod–cone interactions increase the cone-mediated RTs; (2) the rod–cone interactions are strongest when rod sensitivity is maximal in a dark surround, but weaker with increased rod activity in a light surround; and (3) the presence of a dark surround nonselectively increased the mean and variability of chromatic (+L−M, S-cone) and luminance (L + M + S) RTs independent of the level of rod activity. The results demonstrate that lateral rod–cone interactions must be considered when deriving mesopic luminous efficiency using RT.

1. INTRODUCTION

Mesopic illuminations span some three to four log units in natural viewing environments [1]. The combined rod and cone contributions to visual processing under mesopic illuminations result in interactions that alter the sensitivity and perceptual qualities of spatial, temporal, and chromatic vision (for review, see [2]). It is now established that rod signals can access the three primary retinogeniculate pathways as demonstrated in psychophysical studies using a four-primary photostimulator to independently control rod and cone excitations [3–6], and from physiological recordings that detected rod inputs to parasol ganglion cells in the magnocellular (MC) pathways of macaque [7–9] and rhesus [10], to midget ganglion cells of the parvocellular (PC) pathway in macaque [8,9,11,12] and marmoset [13], and to bistratified ganglion cells of the koniocellular (KC) pathway in retina [14,15] and the lateral geniculate nucleus [9] of macaque (but see [8] and [10]). As such, the effect of rod–cone interactions on visual processing appears to be closely linked to the change in activity of the outer and inner retina in response to the temporal, spatial, and spectral properties of the stimuli, the illumination level, and retinal eccentricity.

Reaction time (RT), as a historical measure of visual performance [16,17], has been applied to understand the photopic temporal response properties of chromatic and achromatic processing [18–25] and to determine rod and cone latency differences under mesopic illumination [26–30]. Given the importance of response speed in many real-world applications, RT paradigms are currently being investigated as potential methods for deriving mesopic luminous efficiency functions [29,31–34]. To be used in this application,

*Corresponding author: andrew.zele@qut.edu.au.

RT must be mediated via the MC pathway, the candidate physiological substrate of photopic luminous efficiency function $V(\lambda)$ [35]. In their simplest forms, the models assume that mesopic luminous efficiency is described by a linear combination of the scotopic and photopic luminous efficiency functions [28,29], but the contribution of chromatic opponent processes to mesopic spectral sensitivity are evident in some conditions [33]. If rod–cone interactions alter visual performance within a given level of adaptation, then a system of mesopic photometry based on this method could violate Abney's law of additivity [36].

The effect of lateral rod–cone interactions on visual sensitivity is often studied by comparing the difference in sensitivity to a cone-detected stimulus measured after dark and light adaptation when the test stimulus is set within a dark surround, a spatial configuration that introduces a maximum luminance difference between the test and surround to alter rod and cone sensitivity. In such a paradigm, rods are maximally sensitive in the area outside the test field after dark adaptation and can suppress cone-mediated temporal processing in the test. The observed lateral rod suppression of cone-mediated flicker sensitivity is strongest when the test stimuli have high temporal (8–16 Hz) but low spatial frequency (1–2 cpd) [37]. The dark-adapted rods in the surrounding field attenuate cone-mediated temporal contrast sensitivity at frequencies greater than 6–8 Hz [38] and reduce the critical fusion frequency by ~6 Hz [39]. While the rod–cone interaction across the test and surround fields affects high temporal frequency sensitivity at mesopic light levels; the presence of a luminance difference between the test stimulus and surround field also attenuates photopic temporal contrast sensitivity at low temporal frequencies [40–43]. It is unknown if a dark surround affects mesopic RT.

The aim of this study is to examine the change in cone-mediated, mesopic visual performance in the presence of various rod and cone activities in the test and surround fields. To do this, we use a four-primary photostimulator [44] to independently control rod signaling (with constant cone excitation) and cone signaling (with constant rod excitation) to the inferred MC, PC, and KC pathways with a range of adapting field chromaticities to determine the change in mean RT and the variability of RT.

2. METHODS

A. Apparatus and Calibration Procedures

A four-primary Maxwellian-view photostimulator [44] provided control of the stimulations of the rods and three types of cone photoreceptor classes as described in principle by Shapiro *et al.* [45]. Visual stimuli generated using a four-primary photostimulator are specified with L-cone, M-cone, S-cone, and rod excitations. We normalize rod excitations so that for a light metameric to an equal energy spectrum (EES), 1 photopic Troland (Td) is equal to 1 rod Td [45]. The cone chromaticity is described in a relative cone-Td space, which plots $l = L/(L + M)$ versus $s = S/(L + M)$ [46] with a normalization so that $l = 0.667$ and $s = 1.0$ for an EES light. Note that in a cone-based chromaticity space, luminance is typically specified as $(L + M)$ [46]. Here we used $(L + M + S)$ for cone luminance stimulus specifications because (1) S-cones do not contribute to $V(\lambda)$ and (2) to maintain a constant chromaticity while modulating luminance, S-cone excitation needs to be varied in the same proportion and phase as the L- and M-cone excitations. The four-primary photostimulator can generate isolated photoreceptor excitations (L-cone or M-cone or S-cone or rod excitations) and postreceptoral signals [luminance, $(L + M + S)$ and $(L + M + S + R)$, and chromatic, $L/(L + M)$ and $S/(L + M)$]. The $L + M + S + R$ stimulus is the combined rod and cone luminance stimuli. For example, if a neutral density filter changes luminance then the actual change in photoreceptor excitation is $L + M + S + R$. The four-primary photostimulator can therefore vary either cone-mediated luminance $(L + M + S)$ or rod–cone mediated luminance $(L + M + S + R)$.

The primaries are generated using light-emitting diodes (LEDs) combined with narrowband interference filters yielding dominant wavelengths of 658 nm (red), 561 nm (greenish yellow), 516 nm (green), and 459 nm (blue). The center and surround stimulus fields are imaged in the plane of a 2 mm artificial pupil. The radiances of the primaries are controlled by amplitude modulation of a 20 kHz carrier feeding into an eight-channel, high-definition firewire audio preamplifier (M-Audio ProFire 2626 PreAmp) with a 24 bit digital-to-analog converter (DAC) operating at a sampling rate of 192 kHz. The output of each DAC is demodulated [47] and sent to a voltage to frequency converter that provides 1 µs pulses at frequencies up to 250 kHz to control the LEDs [48]. The preamplifier with demodulator has a precision greater than 16 bits [47]. Stimuli were generated using custom-engineered software driven by an Apple MacPro QuadCore Intel computer.

We compensated for individual differences in prereceptoral filtering between the observer and the CIE 1964 10° standard observer by completing observer calibration procedures at 7.5° temporal eccentricity, the peripheral retinal location of the stimulus field used in the experiments. This observer calibration assumes that the photoreceptor spectral sensitivities of the observer at the primary wavelengths are approximately linear transforms of the standard observer color-matching functions, as has been previously demonstrated [44,49]. This method requires an observer to make a photopic color match between two successively presented primary light combinations (459 and 561 nm matched to 516 and 658 nm) by adjusting the luminance of the 459 nm primary (the 561 nm primary is the reference light), the luminance ratio of the 516 and 658 nm primaries, and the combined luminance of the 516 and 658 nm primaries. To estimate the sensitivity difference between the individual observer and the 10° standard observer, we compare the relative radiances of the four primaries required by the participant at the photopic color match with the theoretical values required by the 10° standard observer [44]. Two additional observations confirm the observer calibration. In the first, a 500 ms, 30% contrast rod pulse is invisible after photopigment bleach and highly conspicuous after dark adaptation. In the second, the cone excitations perceptually matching a 1 Hz, 20% contrast rod pedestal are equivalent to a decrease in $L/[L + M]$, increase in $S/[L + M]$, and an increase in $[L + M]$ (i.e., the test color appearance is blue-greenish and brighter) [3–5]. The physical light calibrations, observer calibration procedures, and applications of the photostimulator are described in detail elsewhere [3,6,44,50–52].

B. Psychophysical Paradigms

A 2° circular test stimulus was set in a 13° circular surround, and a fixation point set the center of the test stimulus at 7.5° eccentricity in the temporal retina. The retinal illuminance of the test field was 2 photopic Td. The data were measured at three adapting chromaticities: one was metameric to the EES [$l = L/(L + M) = 0.667$, $s = S/(L + M) = 1.0$; "white" appearing], the second had a higher $l = L/(L + M)$ than EES [$+l$:$L/(L + M) = 0.70$, $S/(L + M) = 1.0$; "red" appearing], and the third had a higher S-cone excitation than EES [$+s$:$L/(L + M) = 0.667$, $S/(L + M) = 1.1$; "blue" appearing].

RT was measured in response to the onset of a 1 s rapid-ON sawtooth stimulus specified using Weber contrast [27,53]. This sawtooth stimulus minimizes adaptation to the incremental light [27], and the contrast metric is common to the response characteristics of the pathways underlying speeded responses [53]. We do not make direct comparisons between the RTs for stimuli mediated via different pathways because they are measured using different stimulus contrast ranges, there are differential sensitivities to the photoreceptor excitation types, and the irreducible minimums were not determined due to the available instrument contrast gamut. These issues have been considered elsewhere [21–24,53,54].

Six photoreceptor or postreceptoral manipulation conditions were studied: (1) L+ M + S (variable cone luminance with constant rod excitation and cone chromaticity), (2) L + M + S + R (variable rod-cone mediated luminance with in-phase modulation of rod and cone excitations and a constant cone chromaticity), (3) L-cone (variable L-cone excitation therefore both cone chromaticity and luminance were changing, constant M, S, rod excitation), (4) + L–M (variable $l = L/(L + M)$, constant S, rod excitation and constant cone luminance), (5) S-cone (variable S-cone excitation, constant L, M, rod excitation and constant cone luminance), and (6) rod (variable rod excitation, constant L, M, S excitation therefore constant cone chromaticity and cone luminance). Depending on the stimulus conditions, we measured RTs for three to five Weber contrasts ranging between 5% and 80%. For observer 2, the S-cone data could only be measured at the highest S-cone contrast (80% Weber contrast).

To study the effect of rod excitation in the surround (lateral rod–cone interactions) on cone-mediated visual performance, we generated conditions with three levels of rod activity and two surround light levels (light and dark). The spatial properties of the test stimulus field and the rod activity levels for each condition are shown in Fig. 1. In the control equiluminant surround condition (Fig. 1, condition A), the baseline rod excitations in the center and surround fields were equal for all test stimuli. In condition B, the surround field has higher rod excitation than the center field (20% rod surrounding contrast for the +L-M stimuli; 40% rod surrounding contrast for the L + M + S and S stimuli). In condition C, cone-mediated RT is measured in a dark surround; rod sensitivity is maximal in the area outside the stimulus. In condition D, the cone-mediated RT is measured in a dark surround as per condition C, except that participants did not dark adapt and light adapted measurements were recorded within 3 min and 30 s after offset of a 7.1 log Td s bleaching light during the cone plateau of the dark adaption curve. The light source for bleaching was a 240 V, 150 W tungsten halogen lamp (3108°K) with a DA-Lite video vision diffuser (Warsaw, Indiana) that together produced light with a correlated color temperature of 2889°K. The bleaching light was presented for 70 s to produce a rod bleach of ~77% when measured with a 2 mm pupil [55]. The effect of rod contrast in the surround is determined by comparing cone-mediated RTs (L + M + S, +L-M and S) measured in the surround field with higher rod excitation (condition B) and the equiluminant control condition (condition A). The effect of lateral dark-adapted rods on the cone-mediated RTs (L + M + S, +L-M and S) is deter mined by comparison of the data measured with the dark surround after dark adaptation (condition C) and after light adaptation in the bleach condition (condition D). The surround effect is determined by comparison of RTs measured on equiluminant (condition A) and dark surrounds (conditions C and D).

C. Procedure

Observers completed 30 min dark adaptation prior to all conditions except for the photopigment bleach condition [Fig. 1(D)] when data were measured during the cone plateau of the dark adaptation curve following extinction of the bleaching light. In a single session, a stimulus condition was measured at multiple contrasts. The stimulus conditions were randomized within and across sessions. A single run consisted of 30 trials, and a minimum of 100 repeats per condition were recorded for each stimulus contrast (four to five runs per stimulus contrast). For the light-adaptation measurements in condition D, photopigment bleaching was conducted prior to each 30 trial run, and there was an average of four bleaches conducted during each 1 h session.

In each run, the observer's right thumb pressed the RT button to increase the illuminance of the stimulus field by 40% to minimize the Troxler effect [56] and initiate a random fore period (1–5 s) that preceded the onset of the 1 s rapid-ON sawtooth stimulus [27,53]. The

observer was under instruction to release their thumb as quickly as possible when stimulus onset was detected. Upon releasing the button, a 10 kHz continuous sinusoidal signal was interrupted to produce a steady voltage that signaled RT, and the illuminance of the stimulus field decreased by 40%. The response button and preamplifier combination produced lag times less than 100 μs, which would not affect the measured RTs [27].

Observers completed extensive practice sessions prior to data collection. Trials with anticipatory responses (<100 ms) or missed trials (3000 ms after stimulus onset) were discarded, and the condition was repeated on the subsequent trial. RTs 2.5 SD from the mean accounted for less than 3% of the data and were deleted for subsequent analysis [57]. The results report the mean RTs and standard errors exclusive of these outliers. The mean data are described by the best-fitting Piéron function of the form $y = RT0 + kC^B$ where B is the exponent, RT0 is the asymptotic latency, and C represents stimulus contrast.

D. Observers

Two experienced psychophysical observers (1F, 37 years old; 1M, 29 years old) participated in all measurements. Both are normal trichromats as assessed with the Raleigh match and the Farnsworth-Munsell 100-hue test. The Queensland University of Technology Human Research Ethics Committee approved the experimental procedures, and the participants provided informed consent.

3. RESULTS

Figure 2 shows the mean RTs (±standard error of the mean) measured as a function of the Weber contrast of the six stimulus types at three adapting chromaticities (upper panels: EES; middle panels: "+l"; lower panels: "+s") for the two observers (left and right columns). In each figure, the symbols code the different stimulus types (circles: L + M + S; squares: L + M S + R; asterisk: L-cone; upward triangle: +L-M; downward triangle: S-cone; diamond: rod). The +L-M data are defined in Weber contrast to facilitate comparison to the other stimulus types. Overall, the pattern of RT data for the two observers was similar for all stimulus types and adapting chromaticities, with the exception of the S-cone data. The S-cone sensitivity was lower, and the S-cone RTs were slower for observer 2 than for observer 1. All mesopic RTs decreased with increasing stimulus contrast. The averaged Piéron exponent across all stimulus types, three adapting chromaticities, −0.13 and two observers was −0.30 (±0.12 SD, range spanning to −0.32). The coefficient of variation (ratio of the standard deviation to the mean) decreased with increasing contrast from 0.26 to 0.06 (i.e., sub-Poisson variation) across all stimuli and Weber contrasts for the conditions.

To evaluate the effect of rod-cone interactions on cone-mediated RTs, Fig. 3 shows the RTs to the highest contrast measured for the L + M + S (upper row), +L-M (middle row), S-cone (lower row) stimuli at +L-M the EES adapting chromaticity for conditions A to D from the two observers (left and right columns). The effect of surrounding rod contrast on L + M + S, +L-M, and S-cone RT was negligible when compared to the control equiluminant condition (conditions B versus A). Compared to the light bleaching (condition D), dark adaptation (condition C) increased the L + M + S RTs measured on the dark surrounds by an average of 42.5 ms (48 and 37 ms slower for each of the two observers, respectively). For the +L-M or S-cone RTs measured on the dark surrounds, there were no significant differences in dark-or light-adapted RTs for observer 1 (for observer 2, the S-cone data for this condition were not measureable).

Cone-mediated RTs measured with dark surrounds (conditions C and D) were slower than those measured with the equiluminant surround (condition A), irrespective of the level of rod activity in dark surround. The L + M + S RT was 76.5 ms slower with a dark surround

after offset of a bleaching light than with the equiluminant control condition (67 and 86 ms slower for each of the two observers). Similarly, the +L-M RT is 76.5 ms slower with a dark surround after bleaching than with the equiluminant surround (51 and 102 ms slower for each of the two observers). The mean S-cone RT for observer 1 is 151 ms slower on the dark surround after bleaching compared to the equiluminant control condition (for observer 2, the S-cone data were not measurable). The lateral rod-cone interaction further increases the mean $L + M + S$ RTs measured on the dark surround com pared to the equiluminant control (condition C versus A). Table 1 indicates that the coefficient of variation for the same stimulus contrast is larger for RT measured with a dark surround (conditions C and D) than with a light surround that is equiluminant (condition A) or has higher rod contrast (condition B).

4. DISCUSSION

This study measured the mesopic visual performance using six photoreceptor or postreceptoral stimulation conditions designed to target the inferred MC, PC, and KC pathways. RTs for all stimulus conditions decreased with increasing contrast for all adapting chromaticities (Fig. 2). It was determined that lateral rod–cone interactions act to slow the mean RT and are strongest for luminance stimuli. In addition, the presence of a dark surround acts to slow the mean RT, increase the variability of RTs, and is nonselective for luminance and chromatic stimuli. This latter effect is also independent of the level of rod activity in the surround.

The effect of rod–cone interactions on visual performance was studied using a paradigm that alters the level of rod activity in the surround outside the test stimulus (lateral interactions). The similarity of $L + M + S$ and $L + M + S + R$ RTs measured on the equiluminant surround condition (Fig. 2; condition A) is consistent with comparable rod- and cone-impulse response functions at this light level [27,50]. The effect of higher surrounding rod excitations on the cone-mediated RT also was negligible (condition B), indicating that our tested rod contrast cannot alter the cone impulse response function, although dark-adapted rods in the surround can change the amplitude and timing of the cone impulse response function [38]. On the dark surround conditions, the $L + M + S$ RTs are faster after light adaptation than dark adaptation; if the faster RT is due to the bleaching light increasing the photoreceptor time constants, then the difference will be evident in the $+L-M$ and S-cone conditions, but this is not the case (Fig. 3). Therefore, we infer that the increased rod activity in the dark surround generates lateral rod–cone interactions that act to slow LMS-cone RTs by an average of 42.5 ms. This indicates that the effect of lateral rod–cone interactions on visual performance is strongest for stimuli mediated via the inferred MC pathway (i.e., $L + M + S$) with a weak effect on chromatic RTs mediated via the inferred PC ($+L-M$ signaling) and KC pathways (S-cone signaling). It will be necessary, however, to examine the chromatic rod–cone interactions at higher contrasts to fully quantify the effects of rod–cone interactions on chromatic visual performance, but this was not possible within the instrument gamut. Our observations for strong suppressive effects of rod–cone interactions on visual performance occurring for stimuli mediated via the inferred MC pathway is therefore consistent with the findings of studies of pathway-specific effects of lateral rod–cone interactions on the critical fusion frequency [39,50], temporal contrast sensitivity [38], the temporal adaptation response [6], and temporal summation [51,52,58]. Because the relative strength of the rod signal in the postreceptoral pathways is linearly related to rod contrast [4], we anticipate that the strength of the interaction will decrease with increasing light level and with lower contrasts [4], but will vary with changes in the temporal profile of the rod signal [6] with larger effects at durations less than about 75 ms when the rod signal is predominantly mediated via the MC pathway [6].

The effect of the dark surround (dark adapted and light bleaching conditions) on RT was nonselective for the luminance (L + M + S) and chromatic (+L−M, S-cone) stimuli and slowed the mean RTs by an average of ~77 ms (Fig. 3) and increased the RT variability (Table 1). It is well known that there is substantial variation within conditions, and the distribution of RTs is positively skewed. The coefficient of variations for our measurements is consistent with observations that variability generally increases with increases in mean response time [59]. We further demonstrate that the spatial structure of the stimulus affects the variability of mesopic RTs to stimuli mediated by the inferred MC, PC, and KC pathways. It has long been considered that the attenuation in photopic temporal sensitivity at low temporal frequency due to luminance differences between the test and surround [40–43] is a property of the retina [41,60,61]. Eye movements, however, are unlikely to play a role because they enhance low-frequency sensitivity [61–63]. There may be multiple origins for the slower mesopic RTs and the increased variability observed on the dark surrounds. Variability will increase with dark surrounds due to spontaneous activations of the cone photopigment (dark noise), at least for L-cones, as demonstrated in physiological recordings of salamander photoreceptor outer segments [64]. The center-surround receptive field ratio is also lower for cone signaling than for rod, or combined rod and cone signaling in macaque MC ganglion cells under mesopic illumination [7], and so the variability due to noise in the dark surround during cone signaling may be higher. If the presence of a dark surround introduced uncertainty about the position of the stimulus, then the coefficient of variations for our peripheral data should be larger than those determined with photopic, foveated data measured on dark surrounds [65] because positional information is more inaccurate in the peripheral retina than the fovea [66], but the variance is not dissimilar between the peripheral and foveal [65] data. We previously proposed that the principal source of mesopic RT variability is subsequent to the primary visual cortex [27,67]; primate MC cell responses to moderate and high contrast stimuli are highly repeatable [68–70], as are recordings in areas of V1 when eye movements are relatively stable, but under natural viewing conditions that allow eye movements, the variability in the V1 response is in the order of six to tenfold higher [71]. It is likely the spatial context would alter the neural signal accumulation or decision criterion during the perceptual decision process to change the variability of the measured RT.

Mesopic RTs depend on the spectral properties of the light when measured with broadband [72] and narrowband test stimuli [28] whereas photopic RTs are independent of wavelengths for photopically matched stimuli presented on dim backgrounds [19]. This differential mesopic sensitivity to wavelength implies mediation via multiple processes [33] whereas the photopic data are mediated via a single process, likely via the MC pathway. The two spatially dependent processes that slow visual performance may affect real-world visual performance in natural scenes illuminated by automobile and street luminaries against darker backgrounds. On the other hand, the use of peripherally fixated, small test stimuli set within larger surrounds in laboratory experiments [28,29,33,34] is likely to limit the effect of rod–cone interactions that could be present in real-world conditions [e.g., 73], and the two conditions should be commensurate if the same luminous efficiency function is to be used in both environments. There is a similarity in the rod and S-cone mediated RTs in one observer, whereas the rod-mediated RTs are slower in the second observer, and so understanding the role of S-cones in the mediation of RTs at short wavelengths where rods have high sensitivity, and the origin of the differences in the S-cone RTs, will be important for determining the validity of visual performance as a measure of mesopic spectral sensitivity. As such, there is evidence that at low contrasts and with appreciable chromatic signals, mesopic spectral sensitivity is better described with a model incorporating opponent +L−M and S-cone signaling [33].

In conclusion, spatial structure is important for controlling the level of rod–cone interactions that act to reduce mesopic visual performance. These interactions show selectivity for photoreceptor signaling mediated via the inferred MC, PC, and KC pathways, and defining their contributions to mesopic vision will be important for any application of RT in the estimation of mesopic luminous efficiency.

Acknowledgments

REFERENCES

1. CIE. Light as a True Visual Quantity: Principles of Measurement. 1st ed.. Bureau Central de la CIE; 1994. p. TC-1.4Publ. CIE No. 411978/reprint 1994 ed

2. Buck, SL. Rod–cone interactions in human vision. In: Chalupa, LM.; Werner, JS., editors. The Visual Neurosciences. MIT; 2004. p. 863-878.

3. Cao D, Pokorny J, Smith VC. Matching rod percepts with cone stimuli. Vis. Res. 2005; 45:2119–2128. [PubMed: 15845243]

4. Cao D, Pokorny J, Smith VC, Zele AJ. Rod contributions to color perception: linear with rod contrast. Vis. Res. 2008; 48:2586–2592. [PubMed: 18561973]

5. Cao D, Zele AJ, Pokorny J. Chromatic discrimination in the presence of incremental and decremental rod pedestals. Vis. Neurosci. 2008; 25:399–404. [PubMed: 18598409]

6. Zele AJ, Maynard ML, Feigl B. Rod and cone pathway signaling and interaction under mesopic illumination. J. Vis. 2013; 13(1):21, 1–19. [PubMed: 23325348]

7. Cao D, Lee BB, Sun H. Combination of rod and cone inputs in parasol ganglion cells of the magnocellular pathway. J. Vis. 2010; 10(2):11, 1–15. [PubMed: 20462312]

8. Lee BB, Smith VC, Pokorny J, Kremers J. Rod inputs to macaque ganglion cells. Vis. Res. 1997; 37:2813–2828. [PubMed: 9415362]

9. Virsu V, Lee BB. Light adaptation in cells of macaque lateral geniculate nucleus and its relation to human light adaptation. J. Neurophysiol. 1983; 50:864–878. [PubMed: 6631467]

10. Wiesel T, Hubel DH. Spatial and chromatic interactions in the lateral geniculate body of the rhesus monkey. J. Neurophysiol. 1966; 29:1115–1156. [PubMed: 4961644]

11. Lee BB, Pokorny J, Smith VC, Martin PR, Valberg A. Luminance and chromatic modulation sensitivity of macaque ganglion cells and human observers. J. Opt. Soc. Am. A. 1990; 7:2223–2236. [PubMed: 2090801]

12. Purpura K, Tranchina D, Kaplan E, Shapley RM. Light adaptation in the primate retina: analysis of changes in gain and dynamics of monkey retinal ganglion cells. Vis. Neurosci. 1990; 4:75–93. [PubMed: 2176096]

13. Weiss S, Kremers J, Maurer J. Interaction between rod and cone signals in responses of lateral geniculate neurons in dichromatic marmosets (Callithrix jacchus). Vis. Neurosci. 1998; 15:931–943. [PubMed: 9764535]

14. Crook JD, Davenport CM, Peterson BB, Packer OS, Detwiler PB, Dacey DM. Parallel ON and OFF cone bipolar inputs establish spatially coextensive receptive field structure of blue-yellow ganglion cells in primate retina. J. Neurosci. 2009; 29:8372–8387. [PubMed: 19571128]

15. Field GD, Greschner M, Gauthier JL, Rangel C, Shlens J, Sher A, Marshak DW, Litke AM, Chichilnisky EJ. High-sensitivity rod photoreceptor input to the blue-yellow color opponent pathway in macaque retina. Nat. Neurosci. 2009; 12:1159–1164. [PubMed: 19668201]

16. Piéron H. Recherches sur les lois de variation des temps de latence sensorielle en fonction des intensités excitatrices. L 'Année Psychologique. 1914; 20:2–96.

17. Woodrow H. Reaction to the cessation of stimuli and their nervous mechanism. Psychol. Rev. 1915; 22:423–452.

18. Mollon JD, Krauskopf J. Reaction time as a measure of the temporal response properties of individual colour mechanisms. Vis. Res. 1973; 13:27–40. [PubMed: 4681989]

19. Nissen MJ, Pokorny J. Wavelength effects on simple reaction time. Percept. Psychophys. 1977; 22:457–462.

20. Nissen MJ, Pokorny J, Smith VC. Chromatic information processing. J. Exp. Psychol. Hum. Learn. Mem. 1979; 5:406–419.

21. Smithson HE, Mollon JD. Is the S-opponent chromatic sub-system sluggish? Vis. Res. 2004; 44:2919–2929. [PubMed: 15380996]

22. McKeefry DJ, Parry NR, Murray IJ. Simple reaction times in color space: the influence of chromaticity, contrast, and cone opponency. Investig. Ophthalmol. Vis. Sci. 2003; 44:2267–2276. [PubMed: 12714670]

23. O'Donell BM, Barraza JF, Colombo EM. The effect of chromatic and luminance information on reaction times. Vis. Neurosci. 2010; 27:119–129. [PubMed: 20594382]

24. Medina JM, Diaz JA. Postreceptoral chromatic-adaptation mechanisms in the red-green and blue-yellow systems using simple reaction times. J. Opt. Soc. Am. A. 2006; 23:993–1007.

25. Medina JM, Diaz JA. S-cone excitation ratios for reaction times to blue-yellow suprathreshold changes at isoluminance. Ophthalmic Physiolog. Opt. 2010; 30:511–517.

26. Barbur JL. Reaction-time determination of the latency between visual signals generated by rods and cones. Ophthalmic Physiolog. Opt. 1982; 2:179–185.

27. Cao D, Zele AJ, Pokorny J. Linking impulse response functions to reaction time: rod and cone reaction time data and a computational model. Vis. Res. 2007; 47:1060–1074. [PubMed: 17346763]

28. He Y, Bierman A, Rea M. A system of mesopic photometry. Lighting Res. Technol. 1998; 30:175–181.

29. He Y, Rea M, Bierman A, Bullough J. Evaluating light source efficacy under mesopic conditions using reaction times. J. Illum. Eng. Soc. 1997; 26:125–138.

30. Mansfield RJ. Latency functions in human vision. Vis. Res. 1973; 13:2219–2234. [PubMed: 4771191]

31. Walkey HC, Barbur JL, Harlow JA, Hurden A, Moorhead IR, Taylor JA. Effective contrast of colored stimuli in the mesopic range: a metric for perceived contrast based on achromatic luminance contrast. J. Opt. Soc. Am. A. 2005; 22:17–28.

32. Walkey HC, Barbur JL, Harlow JA, Makous W. Measurements of chromatic sensitivity in the mesopic range. Color Res. Appl. 2001; 26:S36–S42.

33. Walkey HC, Harlow JA, Barbur JL. Characterising mesopic spectral sensitivity from reaction times. Vis. Res. 2006; 46:4232–4243. [PubMed: 17014885]

34. Walkey HC, Harlow JA, Barbur JL. Changes in reaction time and search time with background luminance in the mesopic range. Ophthalmic Physiolog. Opt. 2006; 26:288–299.

35. Lennie P, Pokorny J, Smith VC. Luminance. J. Opt. Soc. Am. A. 1993; 10:1283–1293. [PubMed: 8320586]

36. Abney W, Festing ER. Colour photometry. Phil. Trans. R. Soc. London. 1886; 177:423–456.

37. Lange G, Denny N, Frumkes TE. Suppressive rod–cone interactions: evidence for separate retinal (temporal) and extra-retinal (spatial) mechanisms in achromatic vision. J. Opt. Soc. Am. A. 1997; 14:2487–2498.

38. Zele AJ, Cao D, Pokorny J. Rod–cone interactions and the temporal impulse response of the cone pathway. Vis. Res. 2008; 48:2593–2598. [PubMed: 18486960]

39. Cao D, Zele AJ, Pokorny J. Dark-adapted rod suppression of cone flicker detection: evaluation of receptoral and postreceptoral interactions. Vis. Neurosci. 2006; 23:531–537. [PubMed: 16961991]

40. Keesey UT. Variables determining flicker sensitivity in small fields. J. Opt. Soc. Am. 1970; 60:390–398. [PubMed: 5437484]

41. Kelly DH. Flickering patterns and lateral inhibition. J. Opt. Soc. Am. 1969; 59:1361–1365.

42. Spehar B, Zaidi Q. Surround effects on the shape of the temporal contrast-sensitivity function. J. Opt. Soc. Am. A. 1997; 14:2517–2525.

43. Anderson AJ, Vingrys AJ. Multiple processes mediate flicker sensitivity. Vis. Res. 2001; 41:2449–2455. [PubMed: 11483176]

44. Pokorny J, Smithson H, Quinlan J. Photostimulator allowing independent control of rods and the three cone types. Vis. Neurosci. 2004; 21:263–267. [PubMed: 15518198]

45. Shapiro AG, Pokorny J, Smith VC. Cone–rod receptor spaces, with illustrations that use CRT phosphor and light-emitting-diode spectra. J. Opt. Soc. Am. A. 1996; 13:2319–2328.

46. Smith VC, Pokorny J. The design and use of a cone chromaticity space. Color Res. Appl. 1996; 21:375–383.

47. Puts MJ, Pokorny J, Quinlan J, Glennie L. Audiophile hardware in vision science; the soundcard as a digital to analog converter. J. Neurosci. Methods. 2005; 142:77–81. [PubMed: 15652619]

48. Swanson WH, Ueno T, Smith VC, Pokorny J. Temporal modulation sensitivity and pulse detection thresholds for chromatic and luminance perturbations. J. Opt. Soc. Am. A. 1987; 4:1992–2005. [PubMed: 3430210]

49. Sun H, Pokorny J, Smith VC. Brightness induction from rods. J. Vis. 2001; 1(1):4, 32–41.

50. Cao D, Lu YH. Lateral suppression of mesopic rod and cone flicker detection. J. Opt. Soc. Am. A. 2012; 29:A188–A193.

51. Sun H, Pokorny J, Smith VC. Rod–cone interaction assessed in inferred magnocellular and parvocellular postreceptoral pathways. J. Vis. 2001; 1(1):5, 42–54.

52. Zele AJ, Kremers J, Feigl B. Mesopic rod and S-cone interactions revealed by modulation thresholds. J. Opt. Soc. Am. A. 2012; 29:A19–A26. special issue on Color Vision.

53. Zele AJ, Cao D, Pokorny J. Threshold units: a correct metric for reaction time? Vis. Res. 2007; 47:608–611. [PubMed: 17240416]

54. Vassilev A, Murzac A, Zlatkova MB, Anderson RS. On the search for an appropriate metric for reaction time to supra-threshold increments and decrements. Vis. Res. 2009; 49:524–529. [PubMed: 19138700]

55. Rushton WA, Powell DS. The rhodopsin content and the visual threshold of human rods. Vis. Res. 1972; 12:1073–1081. [PubMed: 5043563]

56. Troxler, D. Über das Verschwinden gegebener Gegenstände innerhalb unseres Gezichtskreises. In: Himly, K.; Schmidt, JA., editors. Ophthalmologische Bibliothek. Frommann, Jena; 1804. p. 51-53.

57. Ratliff R. Methods for dealing with reaction time outliers. Psychol. Bull. 1993; 114:510–532. [PubMed: 8272468]

58. Kremers J, Meierkord S. Rod–cone-interactions in deuteranopic observers: models and dynamics. Vis. Res. 1999; 39:3372–3385. [PubMed: 10615502]

59. Wagenmakers EJ, Brown S. On the linear relation between the mean and the standard deviation of a response time distribution. Psychol. Rev. 2007; 114:830–841. [PubMed: 17638508]

60. Kelly DH. Sine waves and flicker fusion. Doc. Ophthalmol. 1964; 18:16–35. [PubMed: 14217806]

61. Zaidi, Q.; Ennis, R.; Cao, D.; Lee, BB. Fast and slow processes in color neurophysiology. 22nd Symposium of the International Colour Vision Society; Winchester, UK. 14–18 July 2013;

62. Keesey UT. Flicker and pattern detection: a comparison of thresholds. J. Opt. Soc. Am. 1972; 62:446–448. [PubMed: 5059979]

63. Levinson J. Fusion of complex flicker II. Science. 1960; 131:1438–1440. [PubMed: 14416313]

64. Rieke F, Baylor DA. Origin and functional impact of dark noise in retinal cones. Neuron. 2000; 26:181–186. [PubMed: 10798402]

65. Medina JM, Diaz JA. 1/f noise in human color vision: the role of S-cone signals. J. Opt. Soc. Am. A. 2012; 29:A82–A95.

66. Ukkonen O, Rovamo J, Nasanen R. Effect of location and orientation uncertainty on rms contrast sensitivity with and without spatial noise in peripheral and foveal vision. Optom. Vis. Sci. 1995; 72:387–395. [PubMed: 7566901]

67. Cao D, Pokorny J. Rod and cone contrast gains derived from reaction time distribution modeling. J. Vis. 2010; 10(2):11, 1–15. [PubMed: 20462312]

68. Croner LJ, Purpura K, Kaplan E. Response variability in retinal ganglion cells of primates. Proc. Natl. Acad. Sci. USA. 1993; 90:8128–8130. [PubMed: 8367474]

69. Sun H, Ruttiger L, Lee BB. The spatiotemporal precision of ganglion cell signals: a comparison of physiological and psychophysical performance with moving gratings. Vis. Res. 2004; 44:19–33. [PubMed: 14599568]

70. Uzzell VJ, Chichilnisky EJ. Precision of spike trains in primate retinal ganglion cells. J. Neurophysiol. 2004; 92:780–789. [PubMed: 15277596]

71. Gur M, Beylin A, Snodderly DM. Response variability of neurons in primary visual cortex (V1) of alert monkeys. J. Neurosci. 1997; 17:2914–2920. [PubMed: 9092612]

72. He, YJ.; Rea, M.; Bierman, A.; Bullough, J. Evaluating light source efficacy under mesopic conditions using reaction times. Iesna Annual Conference Proceedings Technical Papers; 1996. p. 236-257.

73. Akashi Y, Rea MS, Bullough JD. Driver decision making in response to peripheral moving targets under mesopic light levels. Lighting Res. Technol. 2007; 39:53–67.
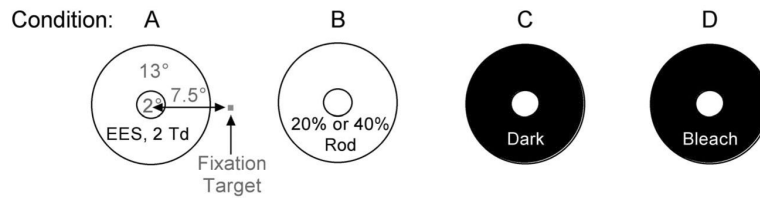
Fig. 1.
Schematic of the spatial configuration used in the four experimental conditions A through D. In all conditions, the 2° diameter test field (2 photopic Td) is positioned at 7.5° temporal eccentricity and set within a 13° diameter surround field. Condition A: rod and cone excitations are equal in the center and surround fields. This is the control equiluminant condition. There are three additional conditions with variable levels of rod activity (B, C, D). Condition B: cone excitations are equal in the center and surround fields, but the surround has higher rod excitation than the center ($+L-M = 20\%$ rod contrast; $L+M+S$ and $S = 40\%$ rod contrast). The surround rod contrast effect is determined by comparison of conditions A and B. Condition C: the dark surround generates maximum rod sensitivity outside the stimulus area to promote lateral rod–cone interactions. Condition D: cone-isolated RTs measured after offset of a bleach light during the cone plateau of the dark-adaptation curve. The effect of rod contrast in the surround is determined by comparing condition B with the control condition A. The effect of lateral rod–cone interaction is determined by comparison of condition C with condition D. The effect of the dark surround is determined by comparison of condition A with conditions C and D.
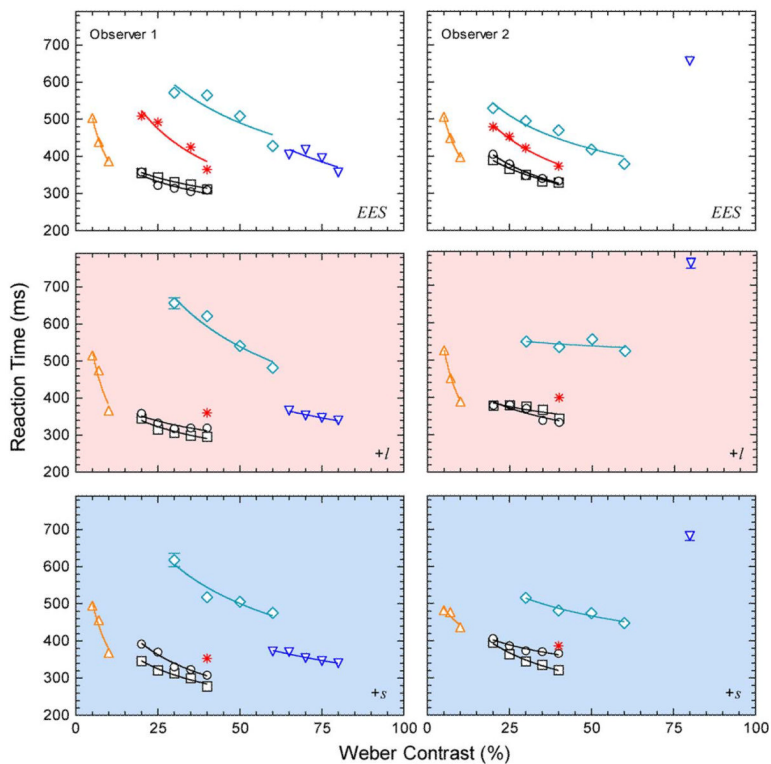
Fig. 2.
RT data for mesopic rod and cone signaling mediated via the inferred MC, PC, and KC pathways. All data were measured in condition A shown in Fig. 1. The left and right columns show the mean RT data (±SEM) for two observers measured on the equiluminant center and surround fields that were metameric to an (EES (upper row), had higher L/(L + M) (middle row) or higher S-cone excitation (lower row). The symbols specify the six photoreceptor excitation conditions: circles (L + M + S: variable cone luminance with a constant rod excitation and cone chromaticity); squares (L + M + S + R: variable rod and cone-mediated luminance with in phase modulation of rod and cone excitations and a constant cone chromaticity); asterisks (L-cone: variable L-cone excitation, therefore both cone chromaticity and luminance were changing, constant M, S, rod excitation); upward triangles (+L-M: variable l = L/(L + M), constant S, rod excitation, and constant cone luminance); downward triangles (S-cone: variable S-cone excitation, constant L, M, rod excitation, and constant cone luminance); diamonds (rod: variable rod excitation, constant L, M, S excitation therefore constant cone chromaticity and cone luminance). The solid lines show the best-fitting Piéron functions.
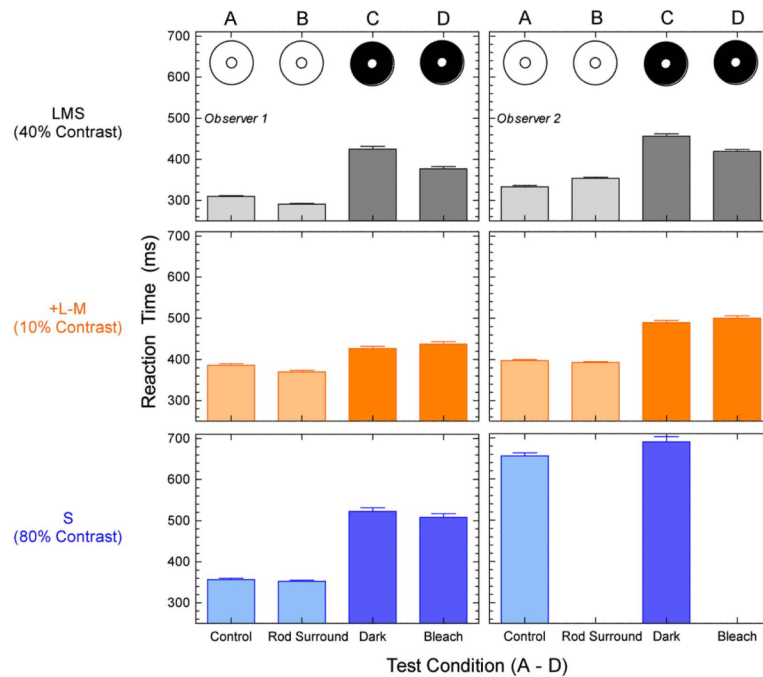
Fig. 3.
Effect of rod–cone interactions on cone-mediated luminance and chromatic RT. The left and right columns show the mean RT data (+SEM) for the two observers at the maximum stimulus contrast measured for the L + M + S stimulus (upper row), the +L-M stimulus (middle row) and the S-cone stimulus (lower row). Data are for the EES adapting chromaticity. The labels and schematics A through D identify the four experimental conditions defined in Fig. 1.

Table 1

Coefficient of Variation of the Luminance (L+M+S) and Chromatic (+L−M, S) RTs Measured on Light and Dark Surrounds

Stimulus	Observer	Light Surround (A, B)		Dark Surround (C, D)	
		Control	+Rod	Dark	Bleach
LMS (40%)	1	0.08	0.08	0.16	0.16
	2	0.11	0.07	0.15	0.12
+L−M (10%)	1	0.10	0.13	0.12	0.15
	2	0.08	0.06	0.11	0.12
S (80%)	1	0.11	0.09	0.19	0.20
	2	0.13	—	0.18	—